International Journal of Modern Physics A
Vol. 32 (2017) 1750065 (17 pages)

DOI: 10.1142/S0217751X17500658

Decoupling the NLO-coupled QED ⊗ QCD, DGLAP evolution equations, using Laplace transform method

Marzieh Mottaghizadeh, Parvin Eslami* and Fatemeh Taghavi-Shahri

Department of Physics, Ferdowsi University of Mashhad, Mashhad, Iran

**eslami@um.ac.ir*

Received 2 October 2016
Revised 28 February 2017
Accepted 23 March 2017
Published 18 April 2017

We analytically solved the QED ⊗ QCD-coupled DGLAP evolution equations at leading order (LO) quantum electrodynamics (QED) and next-to-leading order (NLO) quantum chromodynamics (QCD) approximations, using the Laplace transform method and then computed the proton structure function in terms of the unpolarized parton distribution functions. Our analytical solutions for parton densities are in good agreement with those from CT14QED ($1.295^2 < Q^2 < 10^{10}$) (Ref. 6) global parametrizations and APFEL (A PDF Evolution Library) ($2 < Q^2 < 10^8$) (Ref. 4). We also compared the proton structure function, $F_2^p(x, Q^2)$, with the experimental data released by the ZEUS and H1 collaborations at HERA. There is a nice agreement between them in the range of low and high x and Q^2.

Keywords: Quantum chromodynamics; quantum electrodynamics; perturbative calculations; phenomenological quark models.

PACS numbers: 12.38.−t, 12.20.−m, 12.38.Bx, 12.39.−x

1. Introduction

Accurate determination of the parton distribution function (PDF) inside proton is an essential part of analyzing data in deep-inelastic scattering (DIS) processes.

Precise measurements from high energy hadron colliders such as Tevatron and Large Hadron Collider (LHC) require the inclusion of higher order effects in proton–proton scattering. It seems that the photon-induced Drell–Yan (DY) process such as $\gamma\gamma \to l^+l^-$ has a significant contribution ($\sim 10\%$) to the dilepton invariant mass distribution. Recent results from high mass DY production in ATLAS[1] showed that the contribution of photon distribution inside the proton has the same importance

*Corresponding author.

as the other different PDFs set. To calculate the cross-section of such DY process, one needs to know the photon distribution function inside proton, $\gamma(x, Q^2)$. Furthermore, because the LHC is really a $\gamma\gamma$ collider at very high energy, the determination of photon distribution function inside the proton may be an important issue.

There are a few studies about adding the quantum electrodynamics (QED) corrections to the global parametrizations of PDFs which are based on quantum chromodynamics (QCD) calculations. The first one have been done by the MRST group[2,3] and the other analysis are newly released by NNPDF collaboration[4,5] and CT14QED group.[6]

Here, we will study the analytical solutions for DGLAP evolution equations to obtain the PDFs at next-to-leading order (NLO) QCD and leading order (LO) QED approximations based on the Laplace transform technique which has introduced by Block *et al.*[7–13]

Recently, Khanpour *et al.*[14] calculated the proton structure function and PDFs using the Laplace transform technique at NLO in QCD without QED corrections. They consider the initial value of PDFs from KKT12[15] and GJR08[16] codes at $Q_0^2 = 2$ GeV^2.

The Laplace transform method has an ability that the analytical solutions for the QED $\otimes$ QCD PDFs are obtained more strictly by using the related kernels and the calculations can be controlled well. Following our recent works[17–20] on the analytical solution of DGLAP evolution equations based on the Laplace transform, we have used the same method to solve the QED $\otimes$ QCD DGLAP evolution equations.

The paper is organized as follows. In Sec. 2, we review the QED $\otimes$ QCD-coupled DGLAP evolution equations. In Sec. 3, we bring out the analytical solutions for the DGLAP evolution equations to calculate the PDFs inside the proton based on the Laplace transform. Section 4 is devoted to the results of different kinds of PDFs and also the proton structure function. To be sure about the correctness of our analytical solutions, the final results were cross-checked with the same results from APFEL (A PDF Evolution Library) program and also with the newly released CT14QED code, we selected our initial inputs from CT14QED code at $Q_0 = 1.295$ GeV. Finally, we give our summary and conclusions in Sec. 5.

2. Review of the QED $\otimes$ QCD DGLAP Evolution Equations

The QED $\otimes$ QCD DGLAP evolution equations for the quark, gluon and the photon parton densities can be written as:[21–24]

$$\frac{\partial q_i}{\partial \ln Q^2} = \sum_{j=1}^{n_f} P_{q_i q_j}(x) \otimes q_j + \sum_{j=1}^{n_f} P_{q_i \bar{q}_j}(x) \otimes \bar{q}_j + P_{q_i g} \otimes g + P_{q_i \gamma} \otimes \gamma \,,$$

$$\frac{\partial \bar{q}_i}{\partial \ln Q^2} = \sum_{j=1}^{n_f} P_{\bar{q}_i q_j}(x) \otimes q_j + \sum_{j=1}^{n_f} P_{\bar{q}_i \bar{q}_j}(x) \otimes \bar{q}_j + P_{\bar{q}_i g} \otimes g + P_{\bar{q}_i \gamma} \otimes \gamma \,,$$

$$\frac{\partial g}{\partial \ln Q^2} = \sum_{j=1}^{n_f} P_{gq_j}(x) \otimes q_j + \sum_{j=1}^{n_f} P_{g\bar{q}_j}(x) \otimes \bar{q}_j + P_{gg} \otimes g \,,$$

$$\frac{\partial \gamma}{\partial \ln Q^2} = \sum_{j=1}^{n_f} P_{\gamma q_j}(x) \otimes q_j + \sum_{j=1}^{n_f} P_{\gamma\bar{q}_j}(x) \otimes \bar{q}_j + P_{\gamma\gamma} \otimes \gamma \,, \tag{1}$$

where $q_i(x, Q^2)$, $\bar{q}_i(x, Q^2)$, $g(x, Q^2)$ and $\gamma(x, Q^2)$ are the ith quark, ith antiquark, the gluon and the photon distribution functions, respectively. The $\otimes$ symbol refers to the convolution integral and the splitting functions on the right-hand side of Eq. (22) can be written as

$$\begin{aligned}
P_{q_i\bar{q}_j} &= P_{\bar{q}_i q_j} = a_s^2 \left(\delta_{ij} \, \frac{P_+^{(1)} - P_-^{(1)}}{2} + \frac{P_{qq}^{(1)} - P_+^{(1)}}{2n_f} \right), \\
P_{q_i q_j} &= P_{\bar{q}_i\bar{q}_j} = a_s \delta_{ij} \tilde{P}_{qq}^{(0)} + a_s^2 \left(\delta_{ij} \, \frac{P_+^{(1)} + P_-^{(1)}}{2} + \frac{P_{qq}^{(1)} - P_+^{(1)}}{2n_f} \right) \\
&\qquad + a(\delta_{ij} e_i e_j) \tilde{P}_{qq}^{(0)} \,, \\
P_{gq_i} &= P_{g\bar{q}_i} = a_s P_{gq}^{(0)} + a_s^2 P_{gq}^{(1)} \,, \quad P_{gg} = a_s P_{gg}^{(0)} + a_s^2 P_{gg}^{(1)} \,, \\
P_{\gamma q_i} &= P_{\gamma\bar{q}_i} = a e_i^2 P_{\gamma q}^{(0)} \,, \quad P_{\gamma\gamma} = a P_{\gamma\gamma}^{(0)} \,, \quad P_{q_i\gamma} = P_{\bar{q}_i\gamma} = a e_i^2 \, \frac{P_{q\gamma}^{(0)}}{2n_f} \,.
\end{aligned} \tag{2}$$

The running strong coupling $a_s = \alpha_s/2\pi$ is determined by

$$a_s(Q^2) = \frac{1}{\beta_0 \operatorname{Log}\left(\frac{Q^2}{\Lambda_{\mathrm{QCD}}^2}\right)} \left(1 - \frac{\beta_1}{\beta_0^2} \, \frac{\operatorname{Log}\left(\operatorname{Log}\left(\frac{Q^2}{\Lambda_{\mathrm{QCD}}^2}\right)\right)}{\operatorname{Log}\left(\frac{Q^2}{\Lambda_{\mathrm{QCD}}^2}\right)} \right) \tag{3}$$

and the electromagnetic coupling constant in the recent studies[3] have been considered $\alpha = 1/137$, but here, we give $a = \alpha/2\pi$ as follows:

$$a(Q^2) = \frac{a(\mu^2)}{1 - \frac{38}{9} a(\mu^2) \operatorname{Log}\left(\frac{Q^2}{\mu^2}\right)} \,, \tag{4}$$

where $\beta_0 = \frac{1}{3}(33 - 2n_f)$ and $\beta_1 = 102 - \frac{38}{3} n_f$. For $n_f = 5$, we get $\Lambda_{\mathrm{QCD}} = 0.22$. We suppose $\mu = 1.777$ GeV, then $a(\mu^2) = \frac{1}{2\pi} \frac{1}{133.4}$.[25]

The LO splitting functions are given by[23]

$$\begin{aligned}
P_{qq}^{(0)}(x) &= \frac{4}{3} \left(\frac{1 + x^2}{(1-x)_+} + \frac{3}{2} \, \delta(1-x) \right), \\
\tilde{P}_{qq}^{(0)} = \frac{3}{4} P_{gq}^{(0)} \,, &\quad P_{qg}^{(0)} = n_f \big(x^2 + (1-x)^2 \big) \,, \quad P_{q\gamma}^{(0)} = 2 P_{qg}^{(0)} \,,
\end{aligned}$$

$$P^{(0)}_{\gamma q}(x) = \frac{4}{3}\left[\frac{1+(1-x)^2}{x}\right], \quad P^{(0)}_{\gamma q}(x) = \frac{3}{4}P^{(0)}_{qq}\,,$$

$$P^{(0)}_{gg}(x) = 6\left(\frac{x}{(1-x)_+} + \frac{1-x}{x} + x(1-x) + \left(\frac{11}{12} - \frac{n_f}{18}\right)\delta(1-x)\right),$$

$$\tilde{P}^{(0)}_{\gamma\gamma}(x) = -\frac{2}{3}\sum_{i=1}^{n_f} e_i^2\delta(1-x)\,. \tag{5}$$

The $P^{(1)}_{qq}$, $P^{(1)}_{qg}$, $P^{(1)}_{gq}$ and $P^{(1)}_{gg}$ used in Eq. (2) are the NLO singlet splitting functions, $P^{(1)}_{+}$ and $P^{(1)}_{-}$ are the NLO nonsinglet splitting functions that can be found in Refs. 26 and 27.

For the coupled approach, we utilize a PDF basis for the QED $\otimes$ QCD DGLAP evolution equations, defined by the following singlet and nonsinglet PDF combinations:[28]

$$q^{SG}: \begin{pmatrix} f_1 = \Delta = u+\bar{u}+c+\bar{c}-d-\bar{d}-s-\bar{s}-b-\bar{b} \\ f_2 = \Sigma = u+\bar{u}+c+\bar{c}+d+\bar{d}+s+\bar{s}+b+\bar{b} \\ f_3 = g \\ f_4 = \gamma \end{pmatrix}, \tag{6}$$

$$q^{NS}: \begin{pmatrix} f_5 = d_v = d-\bar{d} \\ f_6 = u_v = u-\bar{u} \\ f_7 = \Delta_{ds} = d+\bar{d}-s-\bar{s} \\ f_8 = \Delta_{uc} = u+\bar{u}-c-\bar{c} \\ f_9 = \Delta_{sb} = s+\bar{s}-b-\bar{b} \end{pmatrix}. \tag{7}$$

We have found that the singlet PDFs evolve as

$$\frac{\partial}{\partial \ln Q^2}\begin{pmatrix} f_1 \\ f_2 \\ f_3 \\ f_4 \end{pmatrix} = \begin{pmatrix} P_{11} & P_{12} & P_{13} & P_{14} \\ P_{21} & P_{22} & P_{23} & P_{24} \\ P_{31} & P_{32} & P_{33} & P_{34} \\ P_{41} & P_{42} & P_{43} & P_{44} \end{pmatrix} \otimes \begin{pmatrix} f_1 \\ f_2 \\ f_3 \\ f_4 \end{pmatrix} \tag{8}$$

and the nonsinglet PDFs, obey the evolution equations such as:

$$\frac{\partial f_i}{\partial \ln Q^2} = P_{ii} \otimes f_i\,, \quad i = 5, \ldots, 9\,. \tag{9}$$

In Eqs. (8) and (9), the new splitting functions are calculated as

$$P_{11} = a_s P^{(0)}_{qq} + a_s^2 P^{(1)}_{+} + \frac{e_u^2 + e_d^2}{2}\, a\tilde{P}^{(0)}_{qq}\,,$$

$$P_{12} = \frac{n_u - n_d}{n_f}\, a_s^2\left(P^{(1)}_{qq} - P^{(1)}_{+}\right) + \frac{e_u^2 - e_d^2}{2}\, a\tilde{P}^{(0)}_{qq}\,,$$

$$P_{13} = \frac{n_u - n_d}{n_f}\left(a_s P^{(0)}_{qg} + a_s^2 P^{(1)}_{qg}\right),$$

$$
\begin{aligned}
P_{14} &= \frac{n_u e_u^2 - n_d e_d^2}{n_f}\, a P_{q\gamma}^{(0)}\,,\\
P_{21} &= \frac{e_u^2 - e_d^2}{2} a \tilde{P}_{qq}^{(0)}\,,\\
P_{22} &= a_s P_{qq}^{(0)} + a_s^2 P_{qq}^{(1)} + \frac{e_u^2 + e_d^2}{2}\, a \tilde{P}_{qq}^{(0)}\,,\\
P_{23} &= a_s P_{qg}^{(0)} + a_s^2 P_{qg}^{(1)}\,,\\
P_{24} &= \frac{n_u e_u^2 + n_d e_d^2}{n_f}\, a P_{q\gamma}^{(0)}\,,\\
P_{31} &= 0\,,\\
P_{32} &= a_s P_{gq}^{(0)} + a_s^2 P_{gq}^{(1)}\,,\\
P_{33} &= a_s P_{gg}^{(0)} + a_s^2 P_{gg}^{(1)}\,,\\
P_{34} &= 0\,,\\
P_{41} &= \frac{e_u^2 - e_d^2}{2}\, a P_{\gamma q}^{(0)}\,,\\
P_{42} &= \frac{e_u^2 + e_d^2}{2}\, a P_{\gamma q}^{(0)}\,,\\
P_{43} &= 0\,,\\
P_{44} &= a P_{\gamma\gamma}^{(0)}\,,\\
P_{55} &= a_s P_{qq}^{(0)} + a_s^2 P_{-}^{(1)} + a e_d^2 \tilde{P}_{qq}^{(0)}\,,\\
P_{66} &= a_s P_{qq}^{(0)} + a_s^2 P_{-}^{(1)} + a e_u^2 \tilde{P}_{qq}^{(0)}\,,\\
P_{77} &= P_{99} = a_s P_{qq}^{(0)} + a_s^2 P_{+}^{(1)} + a e_d^2 \tilde{P}_{qq}^{(0)}\,,\\
P_{88} &= a_s P_{qq}^{(0)} + a_s^2 P_{+}^{(1)} + a e_u^2 \tilde{P}_{qq}^{(0)}\,,
\end{aligned}
\tag{10}
$$

where n_u and n_d are the number of up- and down-type active quark flavors, respectively, and $n_f = n_u + n_d$. In the next section, we try to solve the above equations with Laplace transform method.

3. The Analytical Solutions of the QED ⊗ QCD DGLAP Evolution Equations

Now, we are in a position to briefly review the method of extracting the PDFs via the analytical solutions of DGLAP evolution equations using the Laplace transform technique. Block *et al.*, in Ref. 8, showed that, using the Laplace transform, one can solve the DGLAP evolution equations directly and extract the unpolarized PDFs. We will give the details here and review the method for extracting the unpolarized PDFs of QED⊗QCD-coupled DGLAP equations at LO QED and NLO QCD approximations. By introducing the variables $\nu \equiv \ln(1/x)$ and $\tau\big(Q^2, Q_0^2\big) \equiv \frac{1}{2\pi}\int_{Q_0^2}^{Q^2} \alpha_s(Q'^2) d\ln Q'^2$ into the coupled DGLAP equations, one can turn them into coupled convolution equations in ν and τ spaces. We use two Laplace transforms from ν and τ spaces to s and U spaces, respectively, then the DGLAP equations can be solved iteratively by a set of convolution integrals which are dependent on the unpolarized PDFs at an initial input scale of Q_0^2.

In the following Subsecs. 3.1 and 3.2, we present solutions of Eqs. (8) and (9) separately.

3.1. *The singlet solution*

By considering the variable changes $\nu \equiv \ln(1/x)$ and $w \equiv \ln(1/z)$, one can rewrite Eq. (8) in terms of the convolution integrals as

$$\frac{\partial \hat{F}_i}{\partial \tau}(v,\tau) = \int_0^v \sum_{j=1}^{4} \bigg(\hat{K}_{ij}^{\mathrm{LO,\,QCD}}(v-w) + \frac{\alpha}{\alpha_s}\,\hat{K}_{ij}^{\mathrm{LO,\,QED}}(v-w) + \frac{\alpha_s}{2\pi}\,\hat{K}_{ij}^{\mathrm{NLO,\,QCD}}(v-w)\bigg)\hat{F}_j(w,\tau)dw\,, \quad i = 1,\ldots,4\,. \tag{11}$$

Note that we have used the notation $\hat{F}_i(v,\tau) \equiv F_i(e^{-v},\tau)$. The above convolution integrals show that $\hat{K}_{ij}(v) \equiv e^{-v}P_{ij}(e^{-v})$.

Using this fact that the Laplace transform of a convolution simply is the ordinary product of the Laplace transform of the factors, the Laplace transform from ν space to s space converts Eq. (11) to ordinary first-order differential equations

$$\frac{\partial f_i}{\partial \tau}(s,\tau) = \sum_{j=1}^{4} \bigg(\Phi_{ij}^{\mathrm{LO,\,QCD}} + \frac{\alpha}{\alpha_s}\,\Phi_{ij}^{\mathrm{LO,\,QED}} + \frac{\alpha_s}{2\pi}\,\Phi_{ij}^{\mathrm{NLO,\,QCD}}\bigg) f_j(s,\tau)\,, \quad i = 1,\ldots,4\,. \tag{12}$$

Here, we intend to extend our calculations to the NLO approximation for the Δ, Σ, gluon and photon sectors of unpolarized parton distributions. In this case, to decouple and to solve DGLAP evolution equations (12), we need an extra Laplace transformation from τ space to U space. In the rest of the calculation, the $\alpha_s(\tau)/2\pi$ and $\alpha(\tau)/\alpha_s(\tau)$ are replaced for brevity by $a^{\mathrm{QCD}}(\tau)$ and $a^{\mathrm{QED}}(\tau)$, respectively. Therefore, the solutions of the first-order differential equations in Eq. (12) can be converted to

$$\begin{aligned} UF_i(s,U) - f_{i0}(s) = \sum_{j=1}^{4} \Phi_{ij}^{\mathrm{LO,\,QCD}}(s)F_j(s,U) &+ \Phi_{ij}^{\mathrm{LO,\,QED}}(s)L\big[a^{\mathrm{QED}}(\tau)f_j(s,\tau);U\big] \\ &+ \Phi_{ij}^{\mathrm{NLO,\,QCD}}(s)L\big[a^{\mathrm{QCD}}(\tau)f_j(s,\tau);U\big]\,, \quad i = 1,\ldots,4\,. \end{aligned} \tag{13}$$

To simplify the NLO calculations, we use two excellent approximation relations $a^{\mathrm{QCD}}(\tau) = a_0 + a_1 e^{-b_1\tau}$, where $a_0 = 0.003$, $a_1 = 0.05$ and $b_1 = 4.9$ and also $a^{\mathrm{QED}}(\tau) = -\tilde{a}_0 + \tilde{a}_1 e^{-\tilde{b}_1\tau}$, where $\tilde{a}_0 = -0.0036$, $\tilde{a}_1 = 0.025$ and $\tilde{b}_1 = -3.9$ for $M_b^2 < Q^2 \leq 10^8$ GeV^2.

Therefore, we write expressions $L\big[a^{\mathrm{QCD}}(\tau) f_j(s,\tau); U\big]$ and $L\big[a^{\mathrm{QED}}(\tau) f_j(s,\tau); U\big]$ needed in Eq. (13) as

$$\begin{aligned} L\big[a^{\mathrm{QCD}}(\tau) f_j(s,\tau); U\big] &= \sum_{j=0}^{1} a_j F(s, U + b_j)\,, \\ L\big[a^{\mathrm{QED}}(\tau) f_j(s,\tau); U\big] &= \sum_{j=0}^{1} \tilde{a}_j F(s, U + \tilde{b}_j)\,, \end{aligned} \tag{14}$$

$b_0 = 0$ and $\tilde{b}_0 = 0$.

After introducing the simplified notations for the splitting functions, we will have

$$\Phi_{ij}(s) = \Phi_{ij}^{\mathrm{LO,\,QCD}}(s) + \tilde{a}_0 \Phi_{ij}^{\mathrm{LO,\,QED}}(s) + a_0 \Phi_{ij}^{\mathrm{NLO,\,QCD}}(s)\,, \quad i,j = 1,\ldots,4\,. \tag{15}$$

Therefore, the solutions of the first-order differential equations in Eq. (13) can be changed to

$$\begin{aligned} [U - \Phi_{ii}]\tilde{F}_i(s,U) - \sum_{j=2}^{4} \Phi_{ij} \tilde{F}_j(s,U) \\ = f_{i0}(s) + \tilde{a}_1 \left[\sum_{j=i}^{4} \Phi_{ji}^{\mathrm{LO,\,QED}} F_j(s, U + \tilde{b}_1)\right] \\ + a_1 \left[\sum_{j=i}^{4} \Phi_{ji}^{\mathrm{NLO,\,QCD}} F_j(s, U + b_1)\right], \quad i,j = 1,\ldots,4\,. \end{aligned} \tag{16}$$

The complete solutions of Eq. (16) can be obtained via iteration processes. The iteration can be continued to any required order, but we will restrict ourselves in which we get to a sufficient convergence of the solutions. Our results show that the second-order of iteration is sufficient to get a reasonable convergence. Using the first inverse Laplace transform technique[13] from U space to τ space, we can obtain the following expression for the distributions:

$$f_i(s,\tau) = \sum_{j=1}^{4} k_{ij}(a_1, b_1, s, \tau) f_{j0}(s) \tag{17}$$

with the initial input functions for Σ, Δ, gluon and photon sectors of distributions, which are denoted by $f_{10}(s)$, $f_{20}(s)$, $f_{30}(s)$ and $f_{40}(s)$, respectively. By the second inverse Laplace transform from s space to $\nu \equiv \ln(1/x)$ space, we get PDFs in the usual x space.

3.2. *The nonsinglet solution*

We perform here the nonsinglet solutions of the QED $\otimes$ QCD DGLAP evolution equation (9), using the Laplace transform technique at LO QED and NLO QCD approximations. For the nonsinglet distributions $\hat{F}_i(\nu,\tau)$, after changing to the variable $v \equiv \ln(1/x)$ and the variable τ, we can schematically write Eq. (9) as

$$\frac{\partial \hat{F}_i}{\partial \tau}(\nu,\tau) = \int_0^{\nu} \hat{F}_i(w,\tau) e^{-(\nu-w)} P(\nu-w) dw\,, \quad i=5,\ldots,9\,, \tag{18}$$

where

$$\hat{F}_i(v,\tau) \equiv F_i(e^{-v},\tau)\,, \quad i=5,\ldots,9\,. \tag{19}$$

Going to Laplace space s, we can obtain the first-order differential equations with respect to τ variable for the nonsinglet distributions $f_{i,\mathrm{ns}}(s,\tau)$, whose solutions are

$$f_{i,\mathrm{ns}}(s,\tau) = e^{\tau\Phi_{\mathrm{ns}}(s)} f_{i,\mathrm{ns}\,0}(s)\,, \quad i=5,\ldots,9\,. \tag{20}$$

For example, for valence quarks, such as $U_{\mathrm{val}} = x(u(x,Q^2) - \bar{u}(x,Q^2))$, $\varPhi_{\mathrm{ns}}(s)$ can be written as

$$\Phi_{\mathrm{ns}}(s) = \Phi_{\mathrm{ns}}^{\mathrm{LO,\,QCD}} + \frac{\tau_2}{\tau}\Phi_{\mathrm{ns}}^{\mathrm{LO,\,QED}} + \frac{\tau_3}{\tau}\Phi_{\mathrm{ns}}^{\mathrm{NLO,\,QCD}}\,, \tag{21}$$

where

$$\begin{aligned}
\Phi_{\mathrm{ns}}^{\mathrm{LO,\,QCD}} &= L\left[e^{-v} P_{qq}^{\mathrm{LO}}(e^{-v}); s\right],\\
\Phi_{\mathrm{ns}}^{\mathrm{LO,\,QED}} &= e_u^2 L\left[e^{-v} \tilde{P}_{qq}^{\mathrm{LO}}(e^{-v}); s\right],\\
\Phi_{\mathrm{ns}}^{\mathrm{NLO,\,QCD}} &= L\left[e^{-v} P_{qq}^{\mathrm{NLO}}(e^{-v}); s\right].
\end{aligned}$$

The τ_2 and τ_3 parameters in Eq. (21) are defined as

$$\begin{aligned}
\tau_2 &\equiv \frac{1}{2\pi}\int_0^{\tau} \alpha(\tau') d\ln\tau'\\
&= \frac{1}{(2\pi)^2}\int_{Q_0^2}^{Q^2} \alpha(Q'^2)\alpha_s(Q'^2) d\ln Q'^2\,,\\
\tau_3 &\equiv \frac{1}{2\pi}\int_0^{\tau} \alpha_s(\tau') d\ln\tau'\\
&= \frac{1}{(2\pi)^2}\int_{Q_0^2}^{Q^2} \alpha_s^2(Q'^2) d\ln Q'^2\,.
\end{aligned}$$

The τ_2 parameter is related to the LO QED running coupling constant. The nonsinglet solutions, $f_i(x,Q^2)$, can be obtained using the nonsinglet kernel $K_{\mathrm{ns}}(v) = L^{-1}\left[e^{\tau\Phi_{\mathrm{ns}}(s)}; v\right]$ in the convolution integral

$$\hat{F}_{\mathrm{ns}}(\nu,\tau) = \int_0^{\nu} K_{\mathrm{ns}}(v-w,\tau)\hat{F}_{ns0}(w) dw\,. \tag{22}$$

Table 1. The distributions of xf_{i0} as the initial inputs.

xf_{i0}	
xf_{10}	$(-14767.2x^{1.5}+105659.x^2-3585.68x-0.960083)(1-x)^{2.91524}/(1+20724.9x)$
xf_{20}	$0.28x^{-0.238}(4.967x^{0.5}+1.27x^2+14.98x+1)(1-x)^{3.14}$
xf_{30}	$27.6584x^{0.457605}(1+5.12808x-3.96762x^{0.5}-2.17654x^2)(1-x)^{5.13677}$
xf_{40}	$0.0135x^{-0.0012}(1-x)^{1.14}(1-2.4x^{0.5}+1.49x)$
xf_{50}	$1.18x^{0.568}\left(1+3.8x-4.78x^2\right)(1-x)^{3.73}$
xf_{50}	$1.18x^{0.568}\left(1+3.8x-4.78x^2\right)(1-x)^{3.73}$
xf_{60}	$1.79x^{0.55}(1+5.6x)(1-x)^{3.7}$
xf_{70}	$0.0059x^{-0.416}(1+571.1x-1342.33x^2+2464.27x^{2.5})(1-x)^{4.83}$
xf_{80}	$0.156x^{-0.21}(1+20.12x+2.41x^{0.5}+9.57x^{1.5})(1-x)^{3.03}$
xf_{90}	$0.172x^{-0.184}(1+0.0033x^{0.5})(1-x)^{6.23}$

Finally, with these two Laplace transforms, the evolution equations (22) can be solved iteratively by a set of convolution integrals which are related to the quark distributions at an initial input scale of Q_0^2 in (x, Q^2) space.

4. Results and Discussion

In this section, we will present our results that we obtained for the PDFs and proton structure function, $F_2^p(x, Q^2)$, using the Laplace transform technique. The results are displayed in Figs. 1–5. It should be noted that we need some initial inputs for PDFs, Eqs. (17) and (22). We borrowed data for initial inputs from CT14QED code[6] at $Q_0 = 1.295$ GeV to be sure about the correctness of our solutions. We fit this data with functions in x space and convert these functions by using Laplace transforms from x space to s space and then use them as the initial conditions to get solutions for DGLAP equations. These functions are represented in Table 1. If the solutions are correct, then we expect that our PDFs set and proton structure function have good agreement with those from all global parametrizations (as well as CT14QED) and experimental data.

The valance quark distributions, $xU_{\rm val}(x, Q^2)$ and $xD_{\rm val}(x, Q^2)$, at LO QED and NLO QCD approximations are depicted in Figs. 1 and 2. We also compare them with APFEL model results for the different values of Q^2. The solid curves show our results for the valence quark distributions, and the scatter curves present the APFEL model results. The agreement with both the d and u valance quark distributions, over the large range of x and Q^2, is excellent. The results show that our analytical solutions for the QED⊗QCD DGLAP evolution equations are correct and these solutions are correctly used to calculate the PDFs.

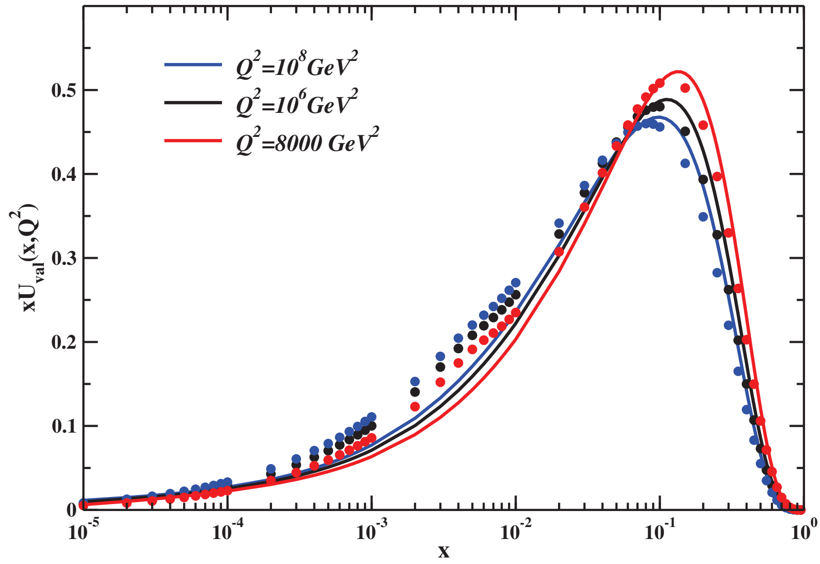

Fig. 1. The $xU_{\mathrm{val}}(x, Q)$ valance quark distributions in different values of Q^2 in comparison with APFEL model.

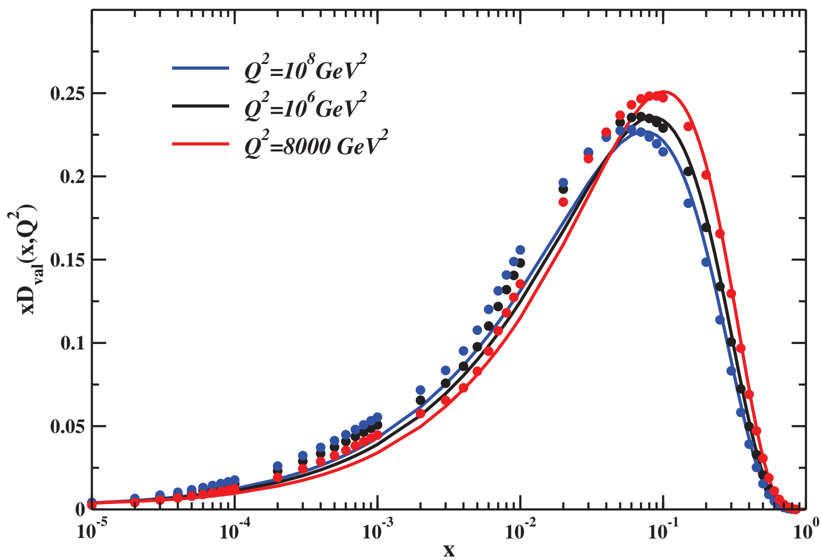

Fig. 2. The $xD_{\mathrm{val}}(x, Q^2)$ valance quark distributions in different values of Q^2 in comparison with APFEL model.

The comparison of photon distribution function, $x\gamma(x, Q^2)$, gluon distribution function, $xg(x, Q^2)$, with APFEL and CT14QED models at $Q^2 = 10^4$ GeV^2 for $\alpha_s\left(Q^2 = M_z^2\right) = 0.118$ is well demonstrated in Fig. 3. This plot indicates that our

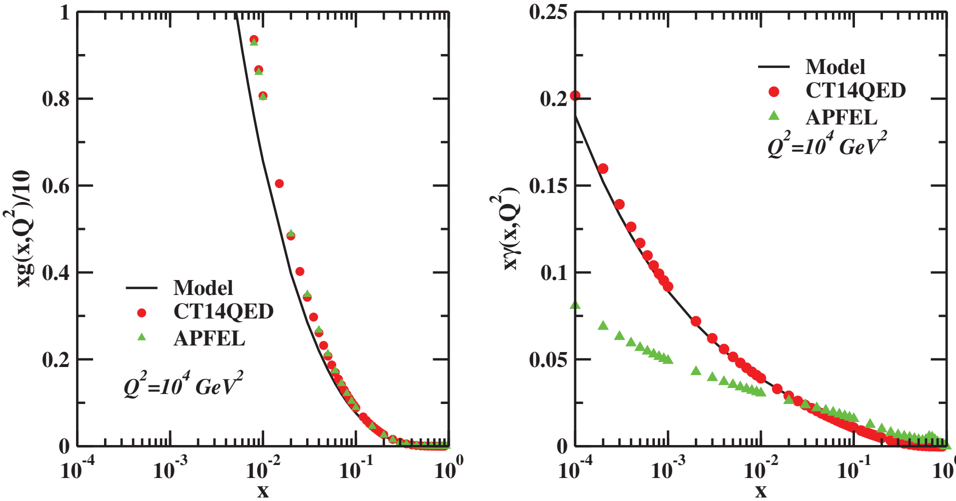

Fig. 3. The photon and gluon distribution functions at $Q^2 = 10^4$ GeV^2 as a function of x in LO QED and NLO QCD approximations in comparison with the available APFEL and CT14QED models.

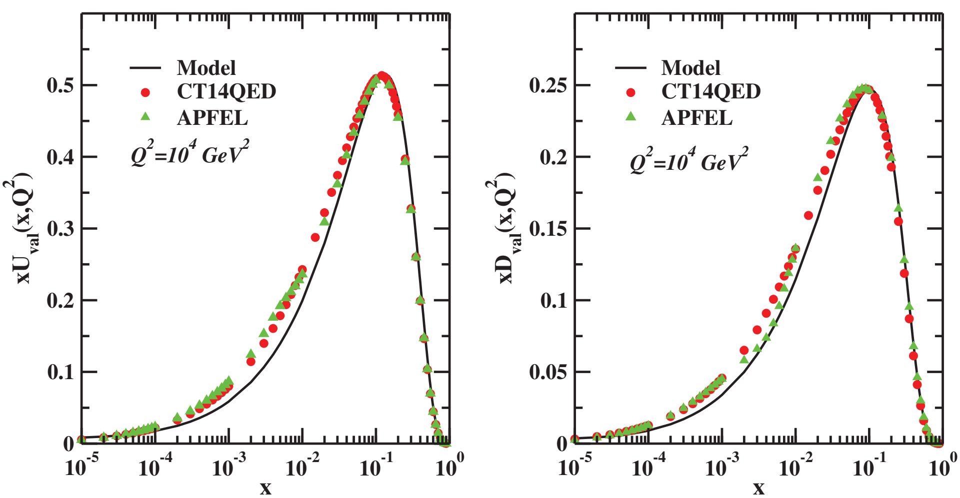

Fig. 4. The comparison of valance quark distributions at $Q^2 = 10^4$ GeV^2 as a function of x with the available CT14QED and APFEL models.

results are in good agreement with APFEL and CT14QED models. Also, it is clear from this figure for photon distribution function that our results in comparison with the CT14QED photon distribution function are very similar at large value of x and are different for small value of x. We also investigate the effect of an increasing value of $Q^2 > Q_0^2$ on the photon distribution functions and conclude that the CT14QED photon distribution function becomes large, whereas our results are distinctly different and much smaller at small values of x (corresponding plot omitted for briefly).

In Fig. 4, we displayed the valance quark distributions at a scale of $Q^2 = 10^4$ GeV^2. We compared those with the APFEL and CT14QED models. It is shown that with increasing the value of Q^2, the contribution of valence quarks are decreased. Therefore, we can conclude that the photon contribution is now significantly considerable.

Figure 5 displays our analytical sea quark distribution functions at $Q^2 = 10^4$ GeV^2. We compared our results with the newly released PDFs global parametrizations from CT14QED[6] and APFEL model. The CT14QED is the first set of CT14 PDFs obtained by including QED evolution at LO with NLO QCD evolution in their global analysis.

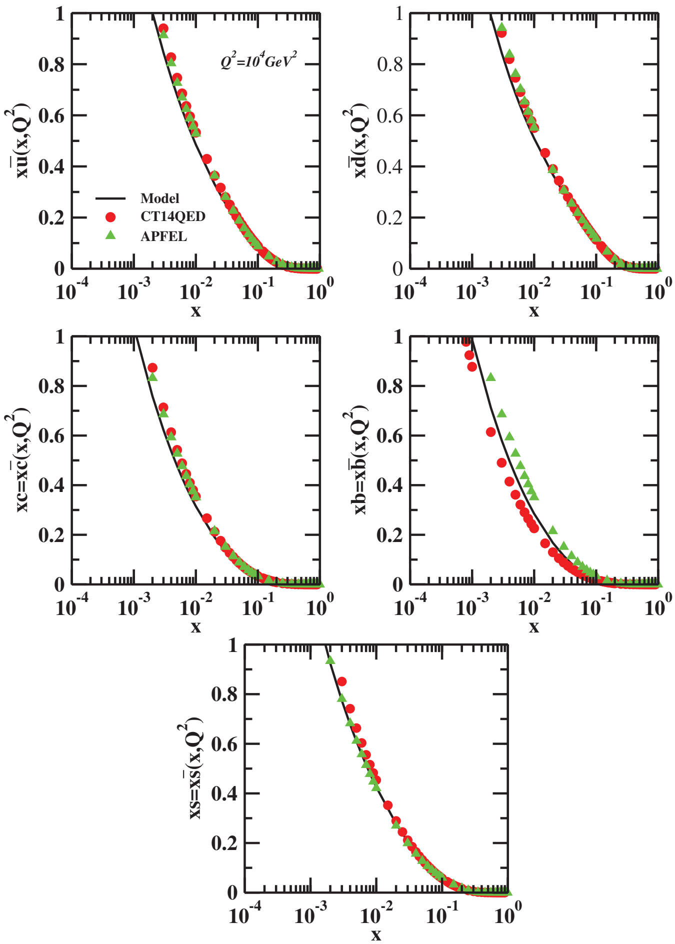

Fig. 5. The comparison of sea quark distributions at $Q^2 = 10^4$ GeV^2 as a function of x in LO QED and NLO QCD approximations with the available CT14QED and APFEL models.

It is found that the sea quark distribution functions in comparison with the photon distribution function in the large values of x with increasing the value of Q^2, contribution of photon is the most significant. It may also be noted that in the range of high x, the photon distribution function is larger than the bottom quark distribution function as with increasing values of Q^2.

It is observed from these figures with increasing the value of Q^2 that the PDFs decrease for the large values of x and increase for the small values of x.

We now proceed by calculating proton structure function. Our aim of investigating the proton structure function is to compare our results with a physical observable that confirm the correctness of our analytical solutions. The Laplace transform technique is also applied to the proton structure function, $F_2^p(x,Q^2)$, which leads to an analytical solution for this function. The method illustrated in this analysis enables us to achieve strictly the analytical solution for proton structure function in terms of x variable.

We will yield the total proton structure functions as $F_2^{p,\,\mathrm{total}}(x,Q^2) = F_2^{p,\,\mathrm{light}}(x,Q^2) + F_2^{\mathrm{heavy}}(x,Q^2)$, where $F_2^{\mathrm{heavy}}(x,Q^2) = F_2^c(x,Q^2) + F_2^b(x,Q^2)$ are the charm and bottom quark structure functions.

For light quarks, the proton structure function $F_2^{p,\,\mathrm{light}}(x,Q^2)$ in Laplace s space, up to the NLO approximation is given by

$$F_2^{p,\,\mathrm{light}}(s,\tau) = F_2^{NS}(s,\tau) + F_2^S(s,\tau) + F_2^G(s,\tau)\,, \tag{23}$$

where the nonsinglet F_2^{NS}, singlet F_2^S and gluon F_2^G contributions are written as

$$\begin{aligned}
F_2^{NS}(s,\tau) &= \left(\frac{4}{9}\,u_v(s,\tau) + \frac{1}{9}\,d_v(s,\tau)\right)\left(1 + \frac{\tau}{2\pi}\,C_q^{(1)}(s)\right),\\
F_2^S(s,\tau) &= \left(\frac{4}{9}\,2\bar{u}(s,\tau) + \frac{1}{9}\,2\bar{d}(s,\tau) + \frac{1}{9}2\bar{s}(s,\tau)\right)\left(1 + \frac{\tau}{2\pi}\,C_q^{(1)}(s)\right),\\
F_2^G(s,\tau) &= \left(\frac{4}{9} + \frac{1}{9} + \frac{1}{9}\right)g(s,\tau)\left(\frac{\tau}{2\pi}\,C_g^{(1)}(s)\right),
\end{aligned} \tag{24}$$

where the $C_q^{(1)}(s)$ and $C_g^{(1)}(s)$ are the NLO Wilson coefficient functions, derived in Laplace s space by $C_q(s) = L\big[e^{-\nu}c_q(e^{-\nu});s\big]$ and $C_g(s) = L\big[e^{-\nu}c_g(e^{-\nu});s\big]$. The NLO Wilson coefficient functions in Bjorken x space are found in Ref. 29. We have found the final desired solution of the proton structure function in x space, $F_2^{p,\,\mathrm{light}}(x,Q^2)$, using the inverse Laplace transform and the appropriate change of variables.

The NLO contribution of heavy quarks, $F_2^{c,b}(x,Q^2)$, to the proton structure function can be calculated in the fixed flavor number scheme (FFNS) approach.[30–36]

The heavy quark structure function, $F_2^{c,b}(x,Q^2) = F_2^{(nl)}(x,Q^2) + F_2^{(d)}(x,Q^2)$, where $F_2^{(nl)}(x,Q^2)$ and $F_2^{(d)}(x,Q^2)$ are the massive-scheme heavy quark structure function and the "difference" contribution, respectively. The Laplace transforms of

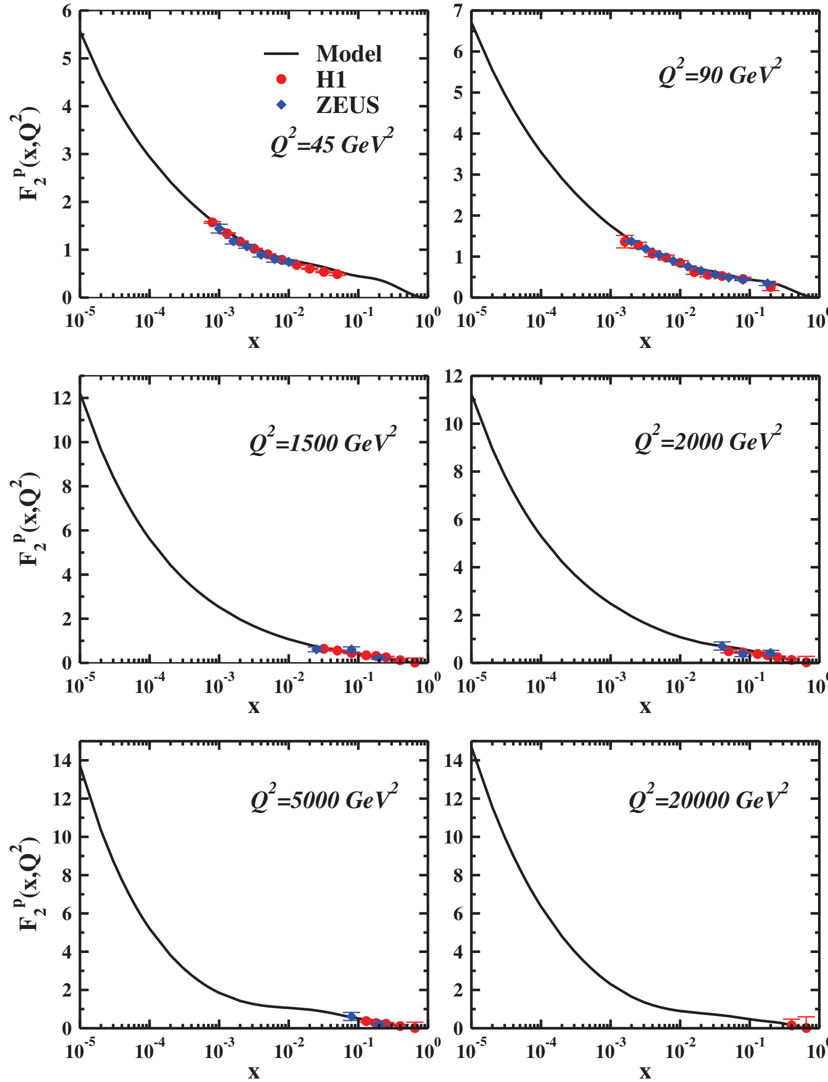

Fig. 6. The proton structure function at $Q^2 = 45$, 90, 1500, 2000, 5000 and 20,000 GeV^2 in comparison with the experimental data.

$F_2^{(nl)}(x, Q^2)$ and $F_2^{(d)}(x, Q^2)$ for charm and bottom quarks are given by

$$F_2^{(nl)}(s,\tau) = \frac{4}{9}\tau\left(C_g^{(1)}(s)\,\mathrm{Log}\left(\frac{Q^2}{m_c^2}\right) + C_g^{(1)}(s)\right)g(s,\tau)\,, \tag{25}$$

$$\begin{aligned} F_2^{(d)}(s,\tau) &= \frac{4}{9}\left(1 + \frac{\tau}{2\pi}C_q^{(1)}(s)\right)(c(s,\tau) + \bar{c}(s,\tau)) \\ &\quad + \frac{4}{9}\,\frac{\tau}{2\pi}\left(C_g^{(1)}(s) - C_g^{(1)}\left(s, m_c^2\right)\right)g(s,\tau) \end{aligned} \tag{26}$$

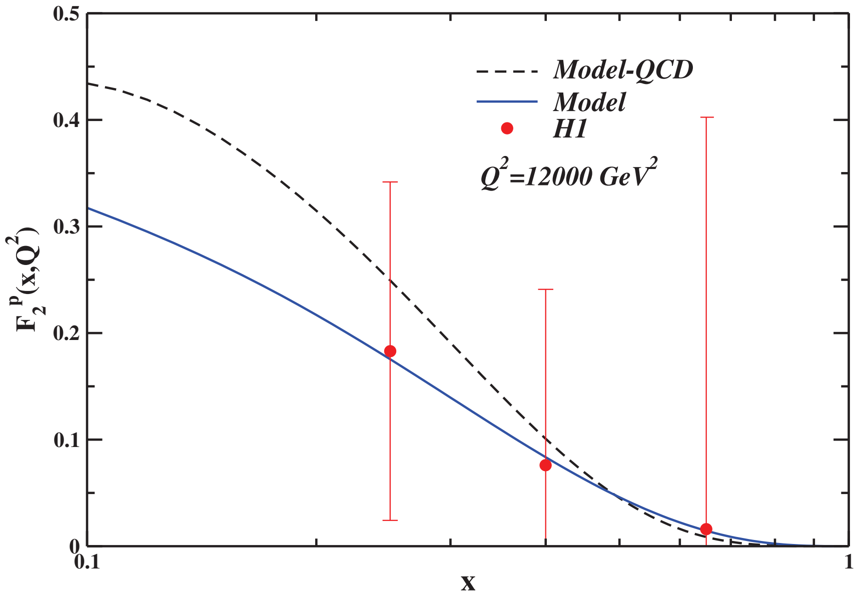

Fig. 7. The proton structure function at $Q^2 = 12{,}000$ GeV^2 in comparison with QCD analysis and experimental data.

and

$$F_2^{(nl)}(s,\tau) = \frac{1}{9}\tau\left(C_g^{(1)}(s)\,\mathrm{Log}\left(\frac{Q^2}{m_b^2}\right) + C_g^{(1)}(s)\right)g(s,\tau)\,, \tag{27}$$

$$\begin{aligned} F_2^{(d)}(s,\tau) &= \frac{1}{9}\left(1 + \frac{\tau}{2\pi}C_q^{(1)}(s)\right)(b(s,\tau) + \bar{b}(s,\tau)) \\ &\quad + \frac{1}{9}\,\frac{\tau}{2\pi}\left(C_g^{(1)}(s) - C_g^{(1)}\left(s, m_b^2\right)\right)g(s,\tau)\,, \end{aligned} \tag{28}$$

where m_c and m_b are the charm and bottom quark masses. The coefficient functions $C_g^{(1)}\left(s, m_c^2\right)$ and $C_g^{(1)}\left(s, m_b^2\right)$ are found in Ref. 37.

Figure 6 depicts the comparison of the proton structure function with the corresponding available experimental data from the H1 and ZEUS Collaborations in the several values of Q^2. The results demonstrate that there is good agreement between them. It is clear that the proton structure function increases with an increase in value of Q^2 for small values of x and decreases for large values of x. All figures indicate that the analytical solutions work well beyond the charm quark mass threshold, $Q^2 > Q_0^2$ ($\approx m_c^2 = 1.677$ GeV^2). Figure 7 displays the comparison of the proton structure function with QED corrections and without these corrections (QCD analysis) with the corresponding experimental data from the H1 Collaboration in the value of $Q^2 = 12{,}000$ GeV^2. This figure shows that the proton structure function with QED corrections is in good agreement with the experimental data in the high energy.

5. Conclusions

In this paper, we utilized the Laplace transform technique to calculate the Laplace transformation of splitting functions and extract the PDFs of quark, antiquark, gluon and photon inside the proton. Our calculations are done in LO QED and NLO QCD approximations. We finally extracted the unpolarized proton structure functions at the different values of Q^2. Our results are compared with APFEL and the newly released CT14QED codes and also with the experimental data which indicate good agreements between them. To determine the proton structure function at any arbitrary Q^2 scale, we only need to know the initial distributions for singlet, gluon, nonsinglet and photon distributions at the input scale of Q_0^2. We borrowed the initial inputs from CT14QED code at $Q_0 = 1.295$ GeV to be sure about the correctness of our solutions. The solutions are seem to be correct because the PDFs and the proton structure function have good agreement with those from all global parametrizations (as well as CT14QED) and experimental data. In the future work with a global parametrization, we can determine these initial inputs. These PDFs can be specifically designed for use in precision cross-section predictions and uncertainties at the LHC.

Acknowledgment

We would like to thank Professor S. Atashbar Tehrani for his help and for the productive discussions.

Appendix. Mathematica Program of the Splitting Functions

Program containing our results for the Laplace transforms of the splitting functions at LO QED and NLO QCD approximations can be obtained via Email from the authors upon request.

References

1. ATLAS Collab. (G. Aad *et al.*), *Phys. Lett. B* **725**, 223 (2013), arXiv:1305.4192 [hep-ex].
2. A. D. Martin, R. G. Roberts, W. J. Stirling and R. S. Thorne, *Eur. Phys. J. C* **4**, 463 (1998), arXiv:hep-ph/9803445.
3. A. D. Martin, R. G. Roberts, W. J. Stirling and R. S. Thorne, *Eur. Phys. J. C* **39**, 155 (2005), arXiv:hep-ph/0411040.
4. V. Bertone, S. Carrazza and J. Rojo, *Comput. Phys. Commun.* **185**, 1647 (2014).
5. NNPDF Collab. (R. D. Ball *et al.*), *Nucl. Phys. B* **877**, 290 (2013), arXiv:1308.0598 [hep-ph].
6. C. Schmidt, J. Pumplin, D. Stump and C. P. Yuan, *Phys. Rev. D* **93**, 114015 (2016).
7. M. M. Block, L. Durand and D. W. Mckay, *Phys. Rev. D* **77**, 094003 (2008).
8. M. M. Block, L. Durand, P. Ha and D. W. McKay, *Eur. Phys. J. C* **69**, 425 (2010), arXiv:1005.2556 [hep-ph].
9. M. M. Block, L. Durand, P. Ha and D. W. McKay, *Phys. Rev. D* **84**, 094010 (2011).
10. M. M. Block, L. Durand, P. Ha and D. W. McKay, *Phys. Rev. D* **83**, 054009 (2011).

11. M. M. Block, *Eur. Phys. J. C* **65**, 1 (2010).
12. M. M. Block, *Eur. Phys. J. C* **68**, 683 (2010).
13. M. M. Block and L. Durand, *Eur. Phys. J. C* **71**, 1806 (2011).
14. H. Khanpour, A. Mirjalili and S. Atashbar Tehrani, *Phys. Rev. C* **95**, 035201 (2017).
15. H. Khanpour, A. N. Khorramian and S. A. Tehrani, *J. Phys. G* **40**, 045002 (2013).
16. M. Gluck, P. Jimenez-Delgado and E. Reya, *Eur. Phys. J. C* **53**, 355 (2008).
17. F. Taghavi-Shahri, A. Mirjalili and M. M. Yazdanpanah, *Eur. Phys. J. C* **71**, 1590 (2011).
18. S. A. Tehrani, F. Taghavi-Shahri, A. Mirjalili and M. M. Yazdanpanah, *Phys. Rev. D* **87**, 114012 (2013).
19. M. Zarei, F. Taghavi-Shahri, S. Atashbar Tehrani and M. Sarbishei, *Phys. Rev. D* **92**, 074046 (2015).
20. S. M. Moosavi Nejad, H. Khanpour, S. Atashbar Tehrani and M. Mahdavi, *Phys. Rev. C* **94**, 045201 (2016).
21. Yu. L. Dokshitzer, *Sov. Phys. JETP* **6**, 641 (1977).
22. V. N. Gribov and L. N. Lipatov, *Sov. J. Nucl. Phys.* **28**, 822 (1978).
23. G. Altarelli and G. Parisi, *Nucl. Phys. B* **126**, 298 (1977).
24. S. Carrazza, arXiv:1509.00209v2 [hep-ph].
25. A. Deur, S. J. Brodsky and G. F. de Teramond, *Prog. Part. Nucl. Phys.* **90**, 1 (2016), arXiv:1604.08082v2 [hep-ph].
26. W. Furmanski and R. Petronzio, *Phys. Lett. B* **97**, 437 (1980).
27. G. Curci, W. Furmanski and R. Petronzio, *Nucl. Phys. B* **175**, 27 (1980).
28. M. Roth and S. Weinzierl, *Phys. Lett. B* **590**, 190 (2004).
29. W. A. Bardeen, A. J. Buras, D. W. Duke and T. Muta, *Phys. Rev. D* **18**, 3998 (1978).
30. M. Gluck, C. Pisano and E. Reya, *Eur. Phys. J. C* **50**, 29 (2007).
31. M. Gluck, C. Pisano and E. Reya, *Eur. Phys. J. C* **40**, 515 (2005).
32. M. Gluck, P. Jimenez-Delgado, E. Reya and C. Schuck, *Phys. Lett. B* **664**, 133 (2008).
33. M. Gluck, E. Reya and M. Stratmann, *Nucl. Phys. B* **422**, 37 (1994).
34. E. Laenen, S. Riemersma, J. Smith and W. L. van Neerven, *Phys. Lett. B* **291**, 325 (1992).
35. S. Riemersma, J. Smith and W. L. van Neerven, *Phys. Lett. B* **347**, 143 (1995).
36. E. Laenen, S. Riemersma, J. Smith and W. L. van Neerven, *Nucl. Phys. B* **392**, 162 (1993).
37. S. Forte, E. Laenen, P. Nason and J. Rojo, *Nucl. Phys. B* **834**, 116 (2010).